

A Photoelastic Fiber-optic Strain Gage

by W. Su, J.A. Gilbert and C. Katsinis

ABSTRACT—This paper reports on the development of a photoelastic fiber-optic strain gage sensitive to transverse strain. The sensing element is made from an epoxy resin which is stress frozen to passively achieve the quadrature condition. Light, emitted from an LED operating at 820 nm, is transmitted to and from the sensing element via multimode fibers and the signal is detected using a dual-channel operational photodiode/amplifier.

This unique combination of optics and electronics produces a fiber-optic sensor having a high signal to noise ratio and a measurement system which is lead-in/out insensitive. Results show that strains on the order of 1 microstrain can be measured over an 800 microstrain range when a dummy gage is used for compensation.

Introduction

In recent years a great deal of interest has been expressed in the development of fiber-optic strain gages designed to be bonded on, or embedded within, engineering materials. Most of these gages fall into one of three categories: the single-mode interferometric fiber-optic gage,¹ the polarimetric high birefringence fiber-optic gage,² or the polarimetric single-mode fiber-optic gage.³

For surface-mounted gages, the single-mode interferometric fiber-optic gage has very high sensitivity to axial strain but is lead-in/out sensitive. In general, polarimetric high birefringence fiber-optic gages are less sensitive to axial strain by approximately two orders of magnitude but have the advantage of lead-in/out insensitivity. A dual wavelength system and sophisticated electronics are required to achieve sensitivities comparable to interferometric gages.⁴ Polarimetric single-mode fiber-optic gages are unique in that they measure radial strain at moderate sensitivities; however, they are lead-in/out sensitive and it is often difficult to maintain the quadrature condition during their operation.

This paper reports on the development of a surface-mounted photoelastic fiber-optic strain gage which is sensitive to transverse strain. The gage has a high signal to noise ratio and the measurement system is lead-in/out insensitive. Results show that strains on the order of 1 microstrain can be measured over an 800 microstrain range when a dummy gage is used for compensation.

W. Su is Graduate Research Assistant, J.A. Gilbert (SEM Member) is Professor, Department of Mechanical and Aerospace Engineering, C. Katsinis is Associate Professor, Department of Electrical and Computer Engineering, University of Alabama in Huntsville, Huntsville, AL 35899.

Paper was presented at the 1992 SEM Spring Conference on Experimental Mechanics held in Las Vegas, NV on June 8–11.

Original manuscript submitted: October 4, 1993. Final manuscript received: June 30, 1994.

The Photoelastic Fiber-optic Strain Gage

Many noncrystalline transparent materials which are ordinarily optically isotropic become anisotropic and display optical characteristics similar to crystals when they are stressed. This phenomenon, known as temporary birefringence, forms the basis for the science of photoelasticity.^{5,6} Photoelastic materials which exhibit this characteristic are commonly analyzed with respect to their stress distributions in a device called a polariscope. The simplest type of polariscope is a dark-field plane polariscope which makes use of two linear polarizers whose axes are crossed with respect to each other. Light is passed through the first polarizer and then through the loaded specimen where it is resolved into two plane-polarized waves which are analyzed by the second polarizer. The resulting intensity observed at each point on the specimen is given by

$$I = I_0 \sin^2 2\theta \sin^2 \alpha / 2 \quad (1)$$

where I_0 is the total light intensity and θ is the angle that the principal stress directions make with respect to the axes of the polarizers. The angular phase difference, α , which occurs as the two-plane polarized waves propagate through the loaded specimen is given by

$$\begin{aligned} \alpha &= \frac{2\pi}{\lambda} (n_1 - n_2)d = \frac{2\pi}{\lambda} C(\sigma_1 - \sigma_2)d \\ &= \frac{2\pi}{f_\sigma} (\sigma_1 - \sigma_2)d \end{aligned} \quad (2)$$

where λ is the wavelength, n is the index of refraction, d is the thickness in the direction of light propagation, C is the stress-optic coefficient, and $f_\sigma = \lambda/C$ is the material fringe value.

Equation (1) shows that there are two separate conditions under which extinction of the light occurs. These correspond to an isochromatic fringe pattern superimposed upon an isoclinic fringe pattern. The isoclinic pattern appears when points on the specimen have their principal stress directions along the polarizers.

A schematic diagram of the photoelastic fiber-optic strain gage is shown in Fig. 1. It consists of a photoelastic cube, two linear polarizers and two optical fibers. Assuming that loads are applied to produce a uniaxial stress state, isoclinics may be eliminated by crossing the polarizers and orienting them at 45 deg with respect to the principal stress directions. For this condition, eqs (1) and (2) become

$$I = I_0 \sin^2 \alpha / 2 \quad (3)$$

and

$$\alpha = \frac{2\pi}{f_\sigma} \sigma d = \frac{2\pi}{f_\sigma} E \epsilon d \quad (4)$$

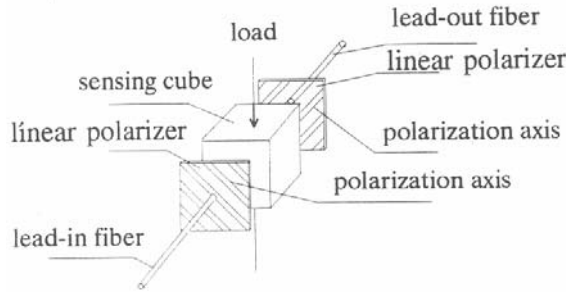


Fig. 1—Basic components of the photoelastic fiber-optic strain gage

where E is the elastic modulus of the photoelastic material and ϵ is the strain in the direction of the applied load.

Equations (3) and (4) show that the output intensity of the photoelastic fiber-optic strain gage is a function of the strain measured in the direction of the applied load and that it fluctuates as the load is varied. Dark fringes are sampled when $\alpha = 2n\pi$; and, the equations may be applied to measure strain simply by counting fringes. However, this approach has a relatively low sensitivity that can be established by taking the properties of the sensing material and the wavelength of the illuminating source into account. That is, the photoelastic fiber-optic strain gage is made of an epoxy resin called PSM-9. The material has a high optical sensitivity (10.5 kPa/fringe/m or 60 psi/fringe/in. at $\lambda = 550$ nm) combined with a reasonably high modulus of elasticity (3.3 GPa or 480×10^3 psi). An LED operating at $\lambda = 820$ nm is used as a light source. The material fringe value at this wavelength can be computed using the relationship $f_\sigma = \lambda/C$, and is equal to 15.7 kPa/fringe/m or 89.5 psi/fringe/in. Assuming a nominal gage length of $d = 6.35$ mm (0.25 in.) and setting $\alpha = 2\pi$ in eq (4), strain is measured at a sensitivity of 746 microstrain/fringe.

An alternative approach is to measure the intensity within a fringe. The change in light intensity ΔI due to a small change in phase $\Delta(\alpha/2)$ can be derived from eq (3) and is given by

$$\Delta I = I_0 \Delta(\alpha/2) \sin \alpha \quad (5)$$

Applying eq (4),

$$\Delta I / \Delta \epsilon = I_0 \left(\frac{\pi E d}{f_\sigma} \right) \sin \left(\frac{2\pi E \epsilon d}{f_\sigma} \right) \quad (6)$$

The photoelastic fiber-optic strain gage can provide a linear output and has the highest sensitivity when the quadrature condition is achieved. This occurs when $\alpha = \pi/2$. In this case, eq (6) reduces to

$$\frac{\Delta I / I_0}{\Delta \epsilon} = \frac{\pi E d}{f_\sigma} \quad (7)$$

The quadrature condition for the sensing element may be passively achieved by stress freezing the photoelastic material.⁵ A tapered tensile specimen can be used to accurately achieve the desired result as described later in the section labeled stress freezing.

Assuming that a photodetector is used to measure the light from the fiber-optic sensor with an output voltage di-

rectly proportional to the light intensity, the system sensitivity, S , can be defined as

$$S = \frac{\Delta V / V_0}{\Delta \epsilon} = \frac{\pi E d}{f_\sigma} \quad (8)$$

For the photoelastic fiber-optic strain gage described, $S = 4212$.

Comparison With Other Types of Strain Gages

Electrical-resistance Strain Gages

The gage factor, S_g , for an electrical-resistance strain gage of resistance R_g and length L is defined as

$$S_g = \frac{dR_g/R_g}{dL/L} = \frac{\Delta R_g/R_g}{\epsilon} = \frac{d\rho/\rho}{\epsilon} + 1 + 2\nu \quad (9)$$

where ρ is the resistivity and ν is the Poisson's ratio. A typical value of S_g for a metallic foil gage is 2.0.

A Wheatstone-bridge circuit is typically used to measure the strain induced change in resistance in terms of a voltage output. Consequently, it is possible to obtain a measure of the system sensitivity for comparison to that of the photoelastic fiber-optic strain gage.

The bridge-circuit sensitivity, S_{cv} , of a single active strain gage in a constant-voltage Wheatstone-bridge circuit is given by the expression⁷

$$S_{cv} = \frac{\Delta V_0}{\Delta R_g/R_g} = \frac{r}{(1+r)^2} V_0 \quad (10)$$

where V_0 is the voltage and r is the resistance ratio.

The overall sensitivity of the Wheatstone bridge is defined in terms of the change in voltage ΔV_0 per unit strain, and is given by the product of the gage factor S_g and the bridge circuit sensitivity S_{cv} . Thus

$$S_s = \frac{\Delta V_0}{\epsilon} = S_g S_{cv} = \frac{\Delta R_g/R_g}{\epsilon} \frac{\Delta V_0}{\Delta R_g/R_g} = S_g \frac{r}{(1+r)^2} V_0 \quad (11)$$

A measure of the system sensitivity comparable to that shown in eq (8) for the photoelastic strain gage, is obtained by dividing each side of eq (11) by V_0 . In that case

$$S = \frac{\Delta V / V_0}{\epsilon} = S_g \frac{r}{(1+r)^2} \quad (12)$$

The circuit efficiency $r/(1+r)$ is limited to the practical range of [50 percent ($r = 1$), 80 percent ($r = 4$), and 90 percent ($r = 9$)] due to the voltage limitations of the power supply.⁷ By substituting $r = 1$ and $S_g = 2.0$ in eq (12), $S = 0.5$. Therefore, the signal from a Wheatstone bridge must be amplified more than 8000 times to achieve the same voltage output as the photoelastic fiber-optic strain gage.

Optical Interferometric Strain Gages

For an optical interferometric strain gage, the phase retardation between the sensing and reference fields propagating along two paths with a difference in length L can be expressed as

$$\phi = \frac{2\pi}{\lambda} nL \quad (13)$$

where n is the index of refraction of the fiber core. The

variation in ϕ due to incremental changes in length is given by the expression

$$\Delta\phi = \frac{2\pi}{\lambda} \left(L \frac{\partial n}{\partial L} \Delta L + n \Delta L \right) = \frac{2\pi}{\lambda} n L \left(1 + \frac{L}{n} \frac{\partial n}{\partial L} \right) \epsilon \quad (14)$$

The equivalent of the gage factor for the interferometric gage is given by

$$S_f = \frac{\Delta\phi/\phi}{\epsilon} = 1 + \frac{L}{n} \frac{\partial n}{\partial L} \quad (15)$$

The second term on the right side of eq (15) is due to the change in index of refraction with strain. For a surface-mounted gage, the second term is small and the value of S_f is approximately equal to 1.0.

The interference produced in the gage can be expressed by eqs (3) and (5) with α replaced by ϕ . Applying eq (13),

$$\Delta I/\Delta\epsilon = I_0 \frac{\pi n L}{\lambda} \left(\frac{\partial n}{\partial L} \frac{L}{n} + 1 \right) \sin \left(\frac{2\pi}{\lambda} n L \right) \quad (16)$$

Assuming that quadrature is maintained and following the argument that the light intensity is directly proportional to the output voltage of the photodetector; the measure of the system sensitivity, S , is

$$S = \frac{\Delta V/V_0}{\epsilon} = \frac{\pi n L}{\lambda} \left(\frac{\partial n}{\partial L} \frac{L}{n} + 1 \right) = S_f \frac{\pi n L}{\lambda} \quad (17)$$

By substituting $S_f = 1.0$, $L = 6.35$ mm (0.25 in.), $n = 1.46$, and $\lambda = 820$ nm in eq (17), $S = 35,519$. Therefore, the signal from the photoelastic strain gage must be amplified eight times to achieve the same voltage output as the interferometric sensor; whereas, the Wheatstone-bridge output must be amplified by a factor of 71,000. The high gain in the optical interferometric strain gage is achieved because the length of the gage is typically several orders of magnitude larger than the wavelength of light.

Experimental

Sensor Design

A preliminary evaluation of the photoelastic fiber-optic strain gage was conducted using the prototype shown in Fig. 2. The gage is mounted on an aluminum substrate so that the sensing element can be easily removed. This allows elements of different size to be tested. The protective cover allows fibers to be easily installed and aligned. Figure 3, on the other hand, shows an experimental setup in which a power supply is used to drive an LED emitting at $\lambda = 820$ nm. Incoherent light from the LED is launched into a

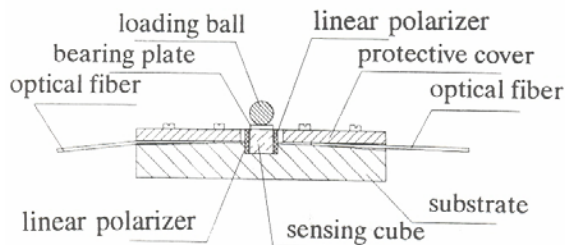


Fig. 2—A prototype of the photoelastic fiber-optic strain gage

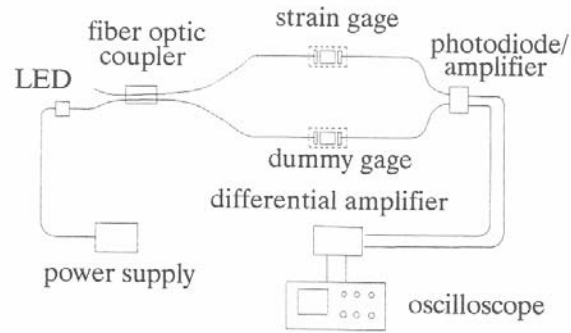


Fig. 3—Experimental setup for testing the photoelastic fiber-optic strain gage

200-micron diameter multimode fiber. The light is split into two similar fibers by a directional coupler. A dummy gage is positioned in one leg of the system while the active gage is positioned in the other leg. The light intensities from these gages are transmitted by 200-micron diameter multimode fibers to the photodetector. The differential amplifier compares these outputs in an effort to reduce noise and minimize environmental effects. The oscilloscope displays the output signal.

According to Sirkis,⁸ most fiber-optic strain gages are sensitive to both axial and transverse strain. They may perform well when surface mounted but when they are embedded, ambiguities may result from triaxial sensitivity. Efforts have been made to minimize these effects. Extrinsic Fabry-Perot sensors,⁹ for example, measure axial strain and are insensitive to transverse strain. The photoelastic fiber-optic strain gage, on the other hand, measures transverse strain and is insensitive to axial strain. This is accomplished by leaving small gaps between the polarizers and the sensing element. The gaps are filled with a matching index fluid to improve the coupling efficiency. The axial strain may introduce a small relative displacement between the fiber leads which may change the coupling efficiency. This effect can be neglected since relatively large core multimode fibers are employed to guide light to and from the sensor and the spacing between fibers is large.

Electro-optic Design and System Components

A high efficiency fiber-optic transmitter containing an etched-well 820-nm $G_{a}AlAs$ emitter was used to couple light into the optical fiber. The transmitter is capable of coupling greater than -10 dB of optical power into a 100/140-micron diameter SMA connector cable assembly. Higher coupling efficiencies were obtained, since light was coupled into an HCS 200/230-micron diameter multimode fiber. The relatively large core and numerical aperture facilitated launching light from the LED into the illuminating fiber and enabled more of the light emitted from the sensor to be transmitted to the electronics. Since the LED produces incoherent light, the photoelastic fiber-optic strain gage is lead in/out insensitive. However, since the output power and wavelength of the LED are temperature related, it must be mounted on an aluminum heat sink to maintain thermal stability.

Specially designed linear polarizers with a thickness of 0.58 mm (0.023 in.) were fabricated. When aligned and

used at a wavelength of 820 nm, the transmission efficiency is 31.5 percent. The transmission efficiency falls to 0.01 percent when the polarizers are crossed.

A considerable amount of light is lost when it is collected from the sensor by the receiving fiber; consequently, a photodetector had to be chosen which could detect optical signals at the microwatt level. This high responsivity was achieved by using a dual-channel operational photodiode/amplifier combination. The unit has a very low noise level; its dual-channel capability facilitated temperature compensation, reduced noise, and helped cancel the effects of variations in LED light intensity during the measurement. An aluminum block was manufactured in order to mount the input fibers and to provide electrical shielding for the electronic circuit. The signal from the photodetector was sent to a differential amplifier and a sum amplifier as shown in Fig. 4. A dual-channel digital oscilloscope was used to acquire, display, and process the signal from the electronic circuit.

Stress Freezing

The method of stress freezing was used to produce a relative retardation in the sensor corresponding to the quadrature condition. The method consists of heating a photoelastic material to a temperature slightly above the softening point or critical temperature followed by slow cooling under load to room temperature.

The 6.35-mm (0.25-in.) \times 6.35-mm (0.25-in.) \times 6.35-mm (0.25-in.) sensing element was cut from the shank of a slightly tapered stress-frozen tensile specimen. The stress in the shank changes as a function of length and the element is cut from the specimen based on the color of the isochromatic fringe pattern observed in a circular polariscope. Table 1 shows the relative retardation and the color corresponding to the first four points which satisfy the quadrature condition (for $\lambda = 820$ nm). Since the first quadrature point is hard to identify, either the second or third quadrature point was selected.

The sensing element was rough cut from the tapered specimen using a band saw and finished to the final dimensions using a milling machine. A high cutting speed and slow feed was used to avoid chipping and overheating during sawing and machining. The finished cube showed good preservation of color (relative retardation) but some residual stresses were introduced close to the free surface.

photodiode/amplifier combination

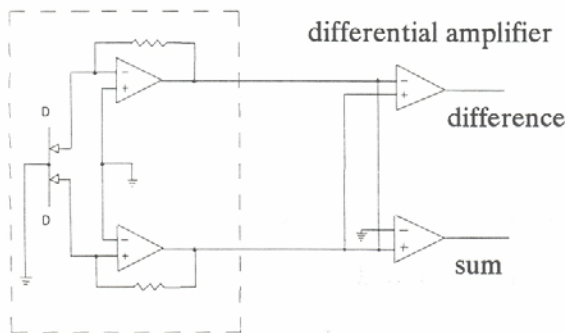


Fig. 4—Circuit diagram of the photodetector

TABLE 1—QUADRATURE POINTS FOR A SENSOR WORKING AT $\lambda = 820$ NM

Point No.	Quadrature Point	Relative Retardation	Color
1	$1/4 \lambda$	205 nm	Gray-White
2	$3/4 \lambda$	615 nm	Deep Blue
3	$1 1/4 \lambda$	1025 nm	Rose Red
4	$1 3/4 \lambda$	1435 nm	Green-Yellow

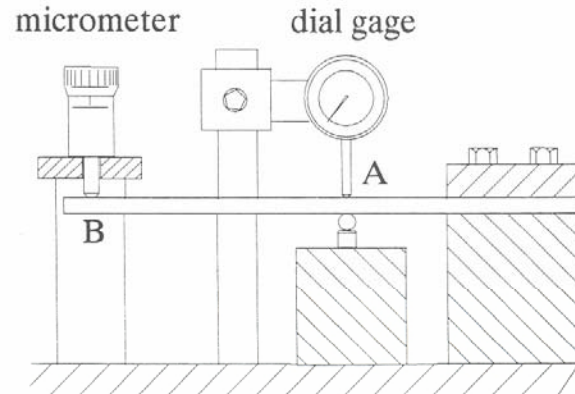


Fig. 5—Test setup for calibrating the prototype

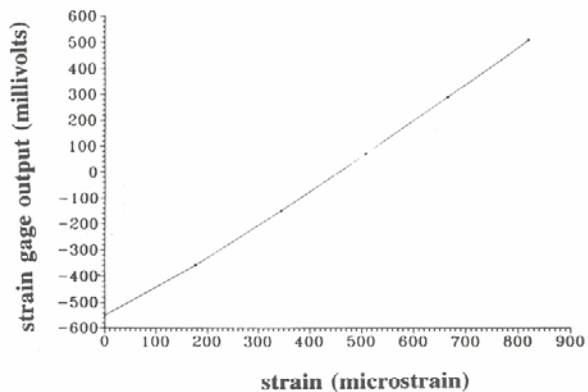


Fig. 6— δ_B versus δ_A (see Fig. 5)

Calibration

The photoelastic fiber-optic strain gage was calibrated using the setup shown in Fig. 5. The gage was mounted on a rigid platform; and, a cantilever beam of length L was positioned above and in contact with it. Deflection was controlled at B using a micrometer having a resolution of 2.54 microns (0.0001 in.). The deflection at point A (located at distance, b , from point B) was monitored using a dial gage. A plot of the deflection applied at B, δ_B , versus the deflection measured at the point of contact, δ_A , is shown in Fig. 6; $\delta_B/\delta_A \approx 45$ when $b/L = 0.75$. The configuration allows deflections on the order of 0.056 microns to be accurately applied to the gage.

These data were used to produce the plot in Fig. 7 which shows the response of the photoelastic fiber-optic strain gage

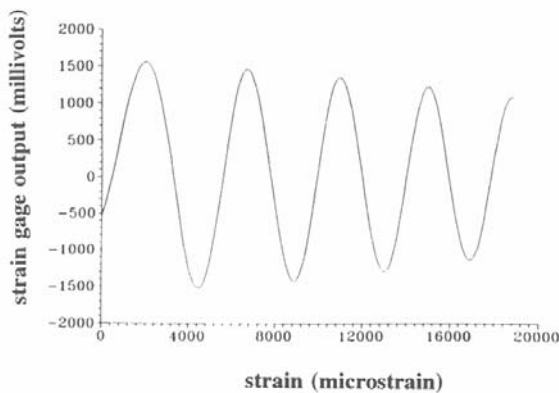


Fig. 7—Sensor output for the fringe-counting method

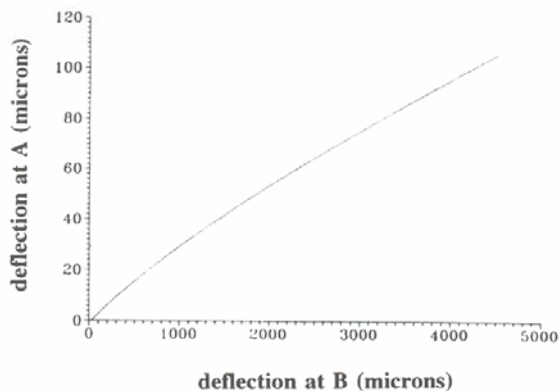


Fig. 8—Sensor output for the quadrature method

to strain. When the fringe counting method is applied, the sensitivity is approximately 4400 microstrain/fringe; nearly six times less than that calculated for a uniaxial stress state. Consequently, when loads are applied to the specimen through the bearing plate, a more complex stress state is produced as a result of the stress concentration which occurs near the free surface. This produces a lower than average strain in the portion of the sensing element through which light is transmitted; thereby, reducing the sensitivity. This contact problem has been studied in detail by Frocht³ using the method of photoelasticity. The stress patterns obtained for "the transmission of a concentrated load through a long plank on an elastic foundation" closely match those observed in the photoelastic fiber-optic strain gage.

Figure 8 shows the trace for the first 800 microstrain. When the quadrature condition is achieved and the sensor is unloaded, the output voltage should be midway between the maximum and minimum voltages shown in Fig. 7. The results show that a slight deviation from the quadrature point occurred; most likely, as a result of the residual stresses introduced while cutting the sensing element from the tapered tensile specimen. The initial response to strain is slightly nonlinear. This is attributed to poor initial contact between the bearing plate and the sensor.

Figure 8 shows that transverse strain can be measured with a sensitivity of approximately $1.31 \text{ mV}/\mu\epsilon$ over 800 microstrain; the dynamic range, defined as the ratio of the range to the resolution, is approximately 30 dB.

Discussion

Results show that the photoelastic fiber-optic strain gage can provide a means for making precise strain measurements. However, the output may be influenced by the conditions of the test environment, the state of strain being measured, and the manner in which the gage is designed and installed.

Since the sensor is a viscoelastic material, it experiences creep and relaxation. Experiments conducted using the photoelastic fiber-optic strain gage and the fringe counting method show that for large strain differences (on the order of several thousand microstrain), creep is significant. However, when the quadrature method is applied and smaller strain differences occur (on the order of several hundred microstrain), the effect produced by creep is minimal. This is illustrated in Fig. 9 which shows a plot of the strain-gage output versus time for a sudden increase in load.

The sensor can be used to monitor a dynamic event when a preload is applied to the sensing element. The upper trace in Fig. 10, for example, shows the response recorded for a seismic loading. The oscilloscope can be adjusted to obtain the power-density spectrum corresponding to the fast Fourier transform (FFT) of the signal received from the sensor. This is illustrated in the lower trace of Fig. 10 which shows the FFT of the output signal.

In any strain-gage-system design, careful consideration must be given to determining whether the change in output is due to applied strain or changes in temperature. In the photoelastic fiber-optic strain gage, the temperature response is influenced by four factors: changes in the material fringe value (f_σ) with temperature; the thermal coefficient of expansion of the sensing cube (α); the thermal coefficient expansion of the substrate (β_1); and, the thermal coefficient of expansion of the specimen (β_2).

The first factor is small when PSM-9 is used close to room temperature. The other factors are much more significant and combine to produce a change in the output of

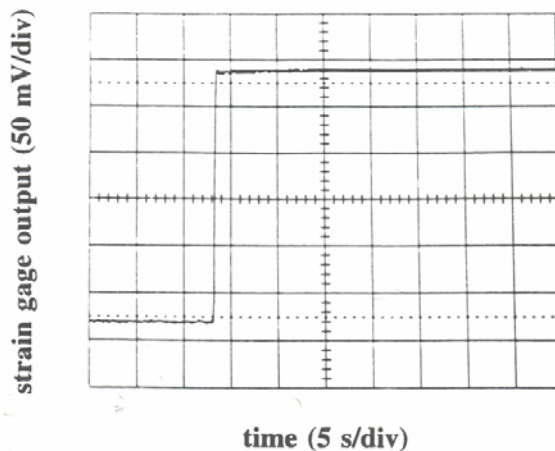


Fig. 9—Sensor output for a sudden increase in load

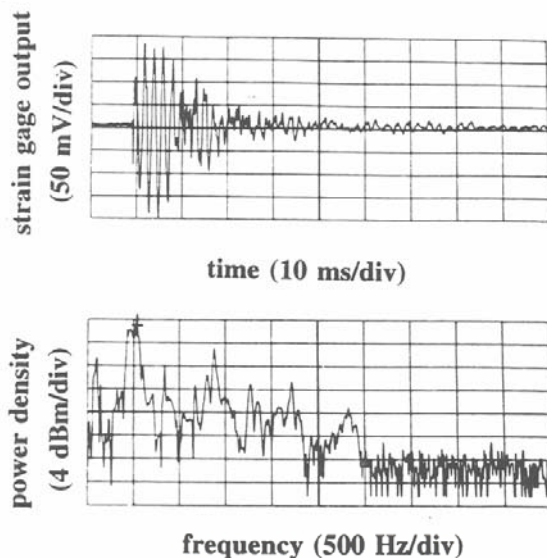


Fig. 10—Sensor output and FFT for a seismic load

the photoelastic fiber-optic strain gage which can be expressed as

$$\left(\frac{\Delta V}{V_0}\right)_{\Delta T} = S\{(\alpha - \beta_1) \Delta T + k(\alpha - \beta_2) \Delta T\} \quad (18)$$

where S is a measure of the system sensitivity as defined in eq (8). The constant, k , has a numerical value ranging from 0 to 1.0 and depends on the offset distance of the fibers above the substrate.

The first term represents the differential expansion between the gage sensing element and the specimen. The second term represents the differential expansion between the sensing element and the aluminum substrate. The thermal coefficient of expansion for metals range from 4.0 to 12.0 PPM/°F. Since the value of the thermal coefficient of expansion of PSM-9 is 39.0 PPM/°F, large thermally induced strains (as much as several hundred microstrain) may result for small changes in temperature (as little as 10°F). Therefore, a dummy gage must be included in the measurement system.

Practical Implementation

The prototype photoelastic fiber-optic strain gage described in this paper is limited; it is relatively large and monitors only compressive strains from its unloaded state. A more practical configuration is schematically illustrated in Fig. 11. The gage is shown upside down. It is designed to be surface mounted by gluing it to the specimen at the two attachment points indicated on the 'I' shaped sensing element. Dimensions are adjusted to create a uniaxial stress state in the sensing region; thereby, making the gage sensitive to transverse strain. To reduce thermally induced strains, the entire gage is fabricated from PSM-9. Fibers leads are located to facilitate alignment and maximize coupling efficiency. With proper design, strains of 1 micro-

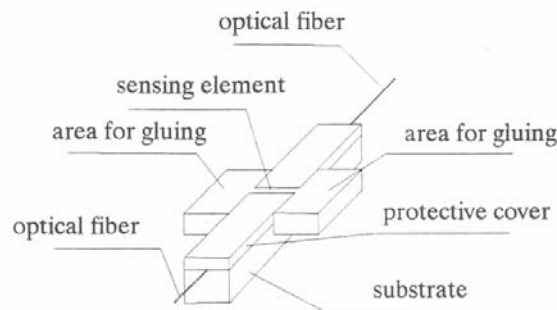


Fig. 11—A more practical version of the photoelastic fiber-optic strain gage

strain can be measured over an extended range (on the order of several hundred microstrain).

Conclusions

A photoelastic fiber-optic strain gage is described with the capability of measuring transverse strains over a range of 800 microstrain to a resolution of 1 microstrain. The sensing element is made from an epoxy resin (PSM-9) which is stress frozen to passively achieve the quadrature condition. Since the system relies on incoherent light and multimode fibers, it is lead in/out insensitive; that is, measurements are unaffected by phase changes caused by perturbations in the optical fiber links.

A comparison with traditional electrical-resistance strain gages shows that the optical amplification associated with the photoelastic gage makes the overall measurement system cost effective. Relatively inexpensive and simple electronics may be employed for production, transmission, and detection of the optical signal. A prototype gage was constructed to compare experimental and theoretical values of strain sensitivity and problems associated with temperature and creep were studied. Guidelines are presented for producing a more practical design.

References

1. Liu, K., Ferguson, M., McEwen, K., Tapanes, E., Measures, R.M., "Acoustic Emission Detection for Composite Damage Assessment Using Embedded Ordinary Single-mode Fiber-optic Interferometric Sensors," *Proc. SPIE*, **1370**, 316-323 (1990).
2. Bock, W.J., Wolinsky, T.R., "Temperature-compensated Fiber-optic Strain Sensor Based on Polarization-rotated Reflection," *Proc. SPIE*, **1370**, 189-196 (1990).
3. Brennan, B.W., "Dynamic Polarimetric Strain Gage Characterization Study," *Proc. SPIE*, **986**, 77-84 (1988).
4. Hogg, W.D., Turner, R.D., Measures, R.M., "Polarimetric Fiber Optic Structural Strain Sensor Characterization," *Proc. SPIE*, **1170**, 542-550 (1989).
5. Frocht, M.M., *Photoelasticity*, II, John Wiley and Sons Ltd. (1948).
6. Kuske, A., Robertson, G., *Photoelastic Stress Analysis*, John Wiley & Sons Ltd. (1974).
7. Kobayashi, A.S., *Handbook on Experimental Mechanics, SEM/Prentice-Hall, Inc.* (1987).
8. Sirkis, J., "Phase-strain-temperature Model for Structurally Embedded Interferometric Optical Fiber Strain Sensors with Applications," *Proc. SPIE*, **1588**, 26-43 (1991).
9. Lesko, J.J., Carman, G.P., Fogg, B.R., Miller, W.V., Vengsarkar, A.M., Reifsnider, K.L., Claus, R.O., "Embedded Fabry-Perot Fiber Optic Strain Sensors in the Macromodel Composites," *Opt. Eng.*, **31** (1) 13-22 (1992).